

**Title (100 characters):** Pulmonary Vascular Compromise is Associated with Survival in Pediatric Pulmonary Hypertension: A New Computational Model

**Authors:** Maria Niccum, MD, MSC<sup>1</sup>, Catherine M. Avitabile, MD<sup>1</sup>, Dana Albizem, CRC<sup>1</sup>, Heather Meluskey, MSN<sup>1</sup>, Christopher Penney<sup>2</sup>, Brian D. Hanna, MD, PhD<sup>1</sup>, Michael L. O'Byrne, MD, MSCE, Zoheir Bshouty, MD, PhD<sup>3,\*</sup>, David B. Frank, MD, PhD<sup>1\*</sup>

**Affiliations:**

<sup>1</sup>Department of Pediatrics, Division of Cardiology, Perelman School of Medicine at the University of Pennsylvania, Children's Hospital of Philadelphia, Philadelphia, PA 19104

<sup>2</sup>Division of Biomedical and Health Informatics, Children's Hospital of Philadelphia, Philadelphia, PA 19104

<sup>3</sup>University of Manitoba, Sections of Respiratory and Critical Care Medicine, RS-317, Respiratory Hospital, 810 Sherbrooke Street, Winnipeg, Manitoba, Canada R3A 1R8

**Short Title (50 characters):** A New Model of Pulmonary Vascular Compromise

**\*Co-corresponding Authors:**

Zoheir Bshouty, MD, PhD, FRCPC  
Associate Professor of Medicine, University of Manitoba  
Attending staff, Sections of Respiratory and Critical Care Medicine  
RS-317, Respiratory Hospital,  
810 Sherbrooke Street, Winnipeg, Manitoba, Canada R3A 1R8  
[ZBshouty@hs.mb.ca](mailto:ZBshouty@hs.mb.ca), [Zoheir.bshouty@umanitoba.ca](mailto:Zoheir.bshouty@umanitoba.ca)

David B. Frank, MD, PhD

27 Children's Hospital of Philadelphia  
28 3615 Civic Center Blvd., ARC 416K  
29 Philadelphia, PA  
30 [frankd@chop.edu](mailto:frankd@chop.edu)

31

32 **Manuscript word count: 3758**

33  
34  
35  
36  
37  
38  
39  
40  
41  
42  
43  
  
44  
  
45  
  
46  
  
47  
  
48  
  
49  
  
50  
  
51  
  
52  
  
53  
  
54  
  
55  
  
56  
  
57

## ABSTRACT:

**Background:** Pediatric pulmonary arterial hypertension (PAH) has a long asymptomatic period with progressive vascular loss. A recent computational model of simulated PAH in humans has demonstrated that up to 70% of the pulmonary vasculature is lost before clinical PAH criteria are met. We sought to evaluate this model in pediatric subjects with PAH and evaluate whether estimated pulmonary vascular compromise (PVC) can predict survival and other clinical outcomes.

**Methods and Results:** Retrospective and prospective cohort data were collected for all subjects with PAH between 1999 and 2022 treated at our center. Cardiac catheterization and clinical data were compared with PVC estimated by the computational model. Transplant-free survival was associated with lower PVC (72% vs 88%,  $p < 0.001$ ). Freedom from transplant/death was also associated with a decrease in PVC over time with no significant change in PVC in subjects who died or underwent transplant. By Kaplan-Meier analysis, 10-year survival was 54% (IQR 35%, 81%) when PVC was more than 80%, compared with 100% survival (IQR 100%, 100%) when PVC was less than 80% ( $p < 0.001$ ). By Cox proportional hazard regression, PVC was associated with mortality (HR 1.1,  $p = 0.008$ ). Lower PVC was associated with better percent predicted 6-minute walk distance (-0.25, 95% CI [-0.35, -0.14],  $p < 0.001$ ), lower log brain natriuretic peptide (0.12, 95% CI [0.07, 0.18],  $p < 0.001$ ), and lower estimated 1-year mortality (0.01, 95% CI [0.01, 0.02],  $p < 0.001$ ).

## Conclusions:

Estimated PVC predicts transplant-free survival and other clinical outcomes in pediatric PAH and provides an adjunctive tool to potentially capture pulmonary vascular loss early in disease.

**Key Words:** Pulmonary arterial hypertension, computational model, survival

## **Clinical Perspective**

### **What Is New?**

- **A new computational model can estimate pulmonary vascular area loss or pulmonary vascular compromise (PVC).**
- **PVC can detect early vascular loss and is associated with transplant-free survival and clinical outcomes in pediatric pulmonary arterial hypertension.**

### **What Are the Clinical Implications?**

- **PVC may detect pulmonary vascular disease early in the disease process and could be used as an adjunct tool for management of patients with pulmonary arterial hypertension.**

## INTRODUCTION

Pulmonary arterial hypertension (PAH) is characterized by aberrant remodeling in the pulmonary vasculature that contributes to a significant loss of the pulmonary vascular bed (1-6). The reduction in vascular area leads to increases in pulmonary vascular resistance (PVR) and pulmonary arterial pressures (PAP). Left untreated, PVR and PAP continue to increase leading to right heart failure and subsequently, death.

Currently, diagnosis, monitoring of treatment response, and risk prediction for PAH requires the use of invasive hemodynamic data and several functional and laboratory parameters. Cardiac catheterization provides information about PAP, pulmonary capillary wedge pressure (PCWP) or left atrial pressure (LAP), right atrial pressure (RAP), pulmonary blood flow (Qp), and PVR (2,4,7,8). New York Heart Association (NYHA) functional class, brain-type natriuretic peptide level (BNP), and 6-minute walk distance (6MW) can be used to non-invasively track progression of disease over time (7,9-13). Despite these advances in disease monitoring and the development of several treatments for PAH improving mortality in the modern era, morbidity and mortality remain high, particularly in patients with idiopathic PAH and repaired congenital heart disease (14-19). This can be explained in part by a period of progressive vascular loss early in the disease course that is asymptomatic and not associated with significant rise in PAP or PVR. In later disease, PAP and PVR begin to rise and right ventricular (RV) failure develops, leading to patient symptoms. Current strategies for monitoring patients with PAH detect disease at this later stage, when irreversible vascular loss has already occurred. Thus, risk prediction early in the disease course remains a significant challenge to improving outcomes, and adjunctive tools to monitor patients with PAH are needed to detect early disease prior to the onset of RV failure.

Computational models of the pulmonary vasculature have been previously described (20-23), and their application and limitations in modeling the pulmonary vasculature in PAH have been extensively reviewed elsewhere (24,25). To date, none of these models have been

used to predict the affected area of compromised vasculature in pediatric patients with PAH. More importantly, computational modeling has yet to be used as a variable in risk assessment. To address this, we adapted a computational model that we previously used to simulate theoretical PAH and predict pulmonary vascular loss or pulmonary vascular compromise (PVC) (26). In simulated PAH, the model demonstrated a hyperbolic relationship between PVC and mean PAP (mPAP) or PVR. In addition, it revealed that mPAP and PVR change very little until the vasculature is significantly compromised. To assess the utility of PVC in pediatric PAH, we examined a cohort of pediatric subjects with PAH at a single institution to determine whether PVC or PVC changes over time could predict transplant-free survival and other clinical outcomes in PAH independent of hemodynamic indicators of right heart failure. We hypothesized that subjects with PAH would demonstrate elevation in PVC early in disease course and that PVC would be associated with mortality and other measures of outcome in PAH.

## **METHODS**

### **Study Population**

A retrospective cohort study was performed including all subjects with a World Health Organization (WHO) Group 1 PAH diagnosis prior to 18 years of age who were between 4 to 22 years of age during the study period of 1/1/1999 to 12/31/2022. Subjects were included if they had at least two hemodynamic evaluations with right heart catheterization at our institution and had at least two years of follow-up after their first catheterization or underwent lung transplant or died prior to this timepoint. Subjects younger than 4 years of age were excluded to ensure that age-dependent pulmonary maturation was complete. Subjects with chronic lung disease were also excluded. To obtain a control population of subjects with nearly normal pulmonary vasculature, we included a random sample of patients with a WHO group 2 PH diagnosis during the study period who ultimately underwent orthotopic heart transplantation (OHT). These

patients undergo serial post-transplant catheterizations and demonstrate quickly improving clinical, hemodynamic, or laboratory evidence of PH by last catheterization (27-30). De-identified data, methods, and code will be shared upon request. The study was approved by the Institutional Review Board of The Children's Hospital of Philadelphia.

## **Data Collection and Study Measures**

Data was collected from an existing PAH database and from review of patient charts. The primary exposure was PVC, and the primary outcome was transplant-free survival from the time of first catheterization.

Secondary outcomes included serum BNP, estimated 1-year mortality (as calculated by the logistic regression equation from Clabby et al. that includes  $RAP \times PVR$  (31)), and 6MW (from which a percent predicted 6MW (PP6MW) (32) was calculated). Covariates included hemodynamic and other associated variables obtained at cardiac catheterization including age at catheterization, body mass index, pulmonary blood flow ( $Q_{pi}$ ), PAP, PCWP or LAP, indexed PVR ( $PVR_i$ ), RAP, and  $RAP \times PVR_i$ . Body mass index (BMI), BNP, and 6MW values within two months of each catheterization date were used. Decisions regarding clinical testing (e.g, the frequency and timing 6MW and BNP) were at the discretion of the care team. Missing data are therefore, inevitable, not likely to be missing at random. Therefore, for analyses on which these depended, case restriction was used. Imputation (or alternative strategies to address missing data) were not attempted.

## **PVC Computational Model**

A computational model of the normal pulmonary circulation based on studies in animals was adapted for use in humans to simulate theoretical PAH in a recently published study by Bshouty (26). This model uses PCWP, cardiac index, and mPAP to generate an estimated pulmonary vascular capacitance as a percentage of what is ideal based on estimated lung size.

From the pulmonary vascular capacitance, a percent pulmonary vascular compromise can be obtained. The methodology, algorithms, and theory behind the original model based on experimental data in dogs are detailed extensively in previous studies (33,34), and the code of the computational program can be found at <https://github.com/AdamMajer/bshouty-lung-model>. Briefly, the model is an abbreviated 5-generation branching system that represents 15 generations of arterial and venous vessels bifurcating from the pulmonary artery (PA) to the left atrium (LA). Each model vessel generation represents 3 generations of real lung vessels given that distensibility is independent of diameter and equal across the pulmonary arterial tree(35-38). In addition, parent to daughter vessel length and diameters for the area and resistance calculations are based on human data from a previous study(39). The model assigns a resistance and vascular area for each branch generation under standardized conditions including a transpulmonary pressure ( $P_{tp}$ ) of zero and vessel transmural pressure ( $P_{tm}$ ) of 35 cm H<sub>2</sub>O. Three sets of data are entered into the computational program. General data includes tolerance or activity level for each calculation and reference point for pressure measurements that is assigned at the LA level. Patient specific data includes height, weight, lung height (P-A diameter at left atrial level), lung compliance (assumed to be normal lung compliance ( $C_L$ ) of 0.317 L/cm H<sub>2</sub>O), and lung volume. Hemodynamic data entered include PCWP, Qp and mPAP at  $P_{ai}$  of zero and a  $P_{pi}$  of -5 cm H<sub>2</sub>O reflecting end-expiration. After computer iteration of a stable solution, output data includes the distribution of individual pulmonary vascular flows, arterial, capillary, and venous resistances across the whole pulmonary circulation. In addition, summary data of vascular area (PVC), mPAP, PVR, upstream (arterial), middle (capillary), and downstream (venous) resistances are generated.

## Statistical Analysis

The overall goal of the analysis was to evaluate PVC as a marker in pediatric PAH, specifically to determine whether PVC and change in PVC were associated with increased



likelihood of death or transplant. Baseline characteristics of the study population were summarized via descriptive statistics. Clinical characteristics were compared using Wilcoxon rank sum and/or Fisher's exact test between transplant-free survivors and non-transplant-free survivors at time of first and last cardiac catheterization and for all cardiac catheterizations. Next, the change in PVC and RAPxPVC from first to last catheterization was compared among transplant-free survivors and subjects who died or underwent transplant via paired-Wilcoxon Rank Sum tests.

PVC was calculated and plotted against mPAP and PVR in a simulated model of PAH and compared with data from our population with PAH. Data from subjects with Group 1 PAH was compared with data from subjects with Group 2 PH. Lorentzian curve fitting to produce trendlines in graphs was computed using Graphpad Prism version 10.2.1 for Windows, GraphPad Software, Boston, Massachusetts, USA, [www.graphpad.com](http://www.graphpad.com).

Non-parametric Kaplan-Meier survival estimates with Log rank test were performed to evaluate differences (p-value <0.05) in median survival times between subgroups. Cut points were determined by the median of each variable from all included catheterizations. Survival hazard ratios were generated via time-varying Cox proportional hazards regression. Time-to-event was defined as the time from first catheterization to death or transplant, or to last follow-up for controls. Due to significant multicollinearity, multivariable analysis was not performed. Univariable and multivariable mixed effects linear regression models were used to evaluate the contribution of PVC and hemodynamic parameters on clinical outcomes including BNP, PP6MW, 1-year estimated mortality, and transplant-free survival while controlling for age at catheterization. One-year mortality estimates were calculated using a forward logistic regression equation from Clabby et al. (31). Log-transformed BNP was used in the analysis to ensure normality. All statistical analyses were performed using R version 4.2.0 (2022-04-22), R Foundation for Statistical Computing, Vienna, Austria, [www.R-project.org](http://www.R-project.org).

## RESULTS

### Study Population

Fifty-eight patients met study criteria (**Table 1**). Patients were followed to a median age of 18.9 years (IQR 15.7, 22.8) with a median follow-up time from first catheterization of 10.8 years (IQR 7.5, 15.4). The median number of cardiac catheterizations per patient was 4 (IQR 3, 6). Of the 58 patients, 45 survived without transplant. Subgroups of Group 1 PAH included idiopathic PAH and congenital heart disease-related PAH. A total of 350 cardiac catheterizations were included.

There was no difference in age at diagnosis between survivors and non-survivors. Median age at death or transplant was 17 years. Baseline patient characteristics at first cardiac catheterization at our institution are presented in **Table 2**. Non-survivors were older at first catheterization. They also had lower PP6MW and higher BNP, mPAP, PCWP/left atrial pressure (LAP), indexed PVR (PVRi), right atrial pressure (RAP), and RAPxPVRi. Similar trends were seen when evaluating data from patients' most recent catheterization or last catheterization prior to lung transplant or death. In addition, non-survivors were older at the time of the last cardiac catheterization (16.7 vs. 13.6 years,  $p=0.02$ ) (**Table S1**). When evaluating data from all cardiac catheterizations combined, similar hemodynamic trends were again demonstrated; non-survivors had significantly higher body mass index (18.0 vs. 16.9 kg/m<sup>2</sup>,  $p=0.047$ ) and lower Q<sub>pi</sub> (3.28 vs 3.87 L/min/m<sup>2</sup>,  $p=0.001$ ) (**Table S2**).

### PVC modeling in pediatric PAH

In our previous report, at a fixed LAP of 7.5 mmHg, stepwise increases of mPAP and PVR demonstrated a curvilinear relationship with PVC (26) (**Figures 1A and 2A**, respectively). In addition, the PVC vs. PVR curve shifts downward and to the right with increasing Q<sub>p</sub>, and the PVC vs. mPAP curve shifts upward and to the left with increasing Q<sub>p</sub>.

To evaluate PVC in actual pediatric patients, data from two patient populations were assessed: 350 cardiac catheterizations from 58 patients with documented Group 1 PAH and 75 cardiac catheterizations from eight control Group 2 PH patients who had undergone OHT with eventual resolution of PH on catheterization. Baseline characteristics and cardiac catheterization data for control patients are shown in **Tables S3-S6**. First, PVC for all patients was plotted vs. either mPAP (**Figure 1B**) or PVRi (**Figure 2B**); the relationship was similar to the simulated PAH model. Using Lorentzian curve fitting to predict Qpi trendlines, we saw a curvilinear relationship that shifted the curves with increased cardiac flow. There were no significant changes in patient mPAP or PVRi until the PVC was more than 70%. Thereafter, mPAP and PVRi rose rapidly with increasing PVC.

There were discrete differences in PVC when comparing patients with PAH and patients post-OHT. In PAH, PVC increased with rising mPAP and PVRi (**Figures 3A and 3B**, blue diamonds). Data from post-OHT patients revealed normal mPAP and PVRi and PVC ranging from zero to 80% (**Figures 3A and 3B**, red squares). No post-OHT patient had PVC greater than 80%. All post-OHT patients with any PVC early after transplantation improved to zero or nearly zero in a periodic but decreasing fashion by the end of our data collection period, as illustrated in an example patient included in **Figure 4**.

In transplant-free survivors, PVC at last catheterization was significantly lower than at first catheterization (66% vs. 77%,  $p=0.02$ ). In non-survivors no difference in PVC was seen between first and last catheterization (88% vs. 88%,  $p=0.94$ ). PVC in transplant-free survivors was lower than PVC in non-survivors at both first and last catheterization ( $p<0.001$  for both, **Table 3**). Similar trends were demonstrated when comparing right ventricular workload responses as estimated by  $RAP \times PVR$  in patients with (26 vs. 44,  $p=0.001$ ) and without transplant-free survival (108 vs. 119,  $p=0.79$ ).

## PVC and Associated Factors as Predictors of Survival

Kaplan-Meier survival curves were generated for PVC, PVRi, mPAP, RAP×PVC, BNP, and PP6MW using data from the first (**Figure S1**) and most recent cardiac catheterization (**Figure 5**). Starting from the most recent catheterization, 10-year survival was estimated at 100% when PVC was less than 80%, compared to 54% survival when PVC was higher than 80% ( $p < 0.001$ ) (**Figure 5A**). Similarly, a PVRi threshold of 8 iWU and a mPAP threshold of 42 mmHg correlated with difference in 10-year survival [100% vs. 61% for PVRi ( $p < 0.001$ ) and 100% vs. 60% for mPAP ( $p < 0.001$ )] (**Figures 5B and 5C**). Ten-year survival estimates also differed with an RAP×PVC threshold of 510 [97% vs. 66% ( $p = 0.002$ )], BNP threshold of 65 pg/ml [94% vs. 68% ( $p = 0.036$ )] and PP6MW threshold of 72% [100% vs. 59%] ( $p < 0.001$ ) (**Figures 5D-F**).

Mortality was not associated with age at diagnosis or Qpi (**Table 4**). Age at catheterization, BNP, PP6MW, RAP, LAP, mPAP, PVRi, RAP×PVRi, PVC, and RAP×PVC all predicted mortality with statistical significance. Hazard ratios were close to 1 for most variables. The most impactful predictors of mortality were age at cardiac catheterization (HR 1.19), RAP (HR 1.22), and Qpi (HR 0.61, but  $p = 0.092$ ).

### **PVC as a Prognostic Factor in Additional Clinical Outcomes**

Univariate mixed model analysis demonstrated that all variables except Qpi are significant predictors of PP6MW, BNP, and estimated 1-year mortality by the Clabby et al regression equation in our pediatric PAH population (**Table 5**). In multivariate mixed models, PVRi, RAP, PP6MW, and log Qpi were associated with estimated 1-year mortality. When PVRi was replaced with PVC, only PVC, RAP, and log Qpi were significant predictors of estimated 1-year mortality (**Table 6**).

## **DISCUSSION**

In this single center retrospective cohort study, we demonstrated that a computational model can be applied to quantify progressive pulmonary vascular loss in pediatric patients with PAH, and that worsening PVC was consistently associated with worse transplant-free survival. Consistent with an estimate in a theoretical PAH model by Bshouty (26), PVC greater than 70% indicated severe PAH. Furthermore, PVC was significantly associated with mortality in pediatric PAH. Given this data, the model's simple interface, and iterations taking seconds to predict PVC, any clinician with patient hemodynamic data can employ this adjunctive diagnostic tool for PAH.

This addresses a critical challenge in the chronic treatment of young patients with PAH. PAH is a silent and severe disease. Early detection is difficult as patients with mild disease are often asymptomatic or present with nonspecific symptoms. Diagnosis is often delayed for years, during which vascular remodeling causes lasting and sometimes irreversible damage to the vascular bed (5,18,40,41). The results of the current study may provide a pathophysiologic explanation for this early asymptomatic period. In our model, mPAP and PVRi change very little until 70% of the pulmonary vascular bed is lost. After crossing the 70% threshold of PVC, both mPAP and PVRi rapidly rise, leading to RV hypertension and ultimately symptomatic RV failure. Current World Symposium of PH diagnostic criteria for PAH requires mPAP greater than 20 mmHg, PVRi greater than 3 iWU, and PCPW or LAP less than 15 mmHg. While these criteria identify patients with significant PAH, there is likely a distinct group of patients with early disease, mild disease, or concurrent left-sided disease who are excluded from the definition. The model presented here provides an adjunctive diagnostic tool to identify PAH at an earlier stage and in patients with concurrent left-sided heart disease.

PAH is marked by both fixed and reversible vaso-occlusive lesions that worsen over time. As the disease progresses, the area of functional pulmonary vasculature is reduced. These phenomena have been reported in earlier studies examining biopsies of affected lungs (2,4,12,42). Recent advances in computed tomography (CT) and magnetic resonance imaging

(MRI) have provided some insight into this process as well (43,44). MRI-based pulmonary blood flow analysis can measure perfusion changes in PAH and infers that there is a reduction in the functional pulmonary vasculature (43,45). However, these imaging modalities are limited in the resolution to delineate distal pre-capillary arterioles. Computational modeling to estimate vascular area can provide a reasonable alternative until improved resolution in CT or MRI develops. While lung biopsy can provide information about the degree of disease in distal arterioles, it is significantly more invasive than computational modeling, and detection of patchy disease is difficult due to sampling limitations.

The current study demonstrated that PVC and RAP×PVC are significant predictors of clinical variables such as BNP and PP6MW. Both BNP and PP6MW have been used to monitor clinical response to PAH therapy in multiple small clinical trials (46-51). There is also some evidence that BNP correlates with WHO Functional Class in children with PH (52), and a BNP less than 50 pg/ml is associated with improved survival in children with PAH (14). While BNP and RAP are reflective of a failing RV and increased mortality risk, PVC and the hemodynamic variables required to calculate it are independent of RV function. Thus, PVC is a potential adjunctive tool for the evaluation of PAH.

In this study, PVC and RAP×PVC were associated with both estimated and actual mortality. PVC and RAP×PVC were associated with estimated 1-year mortality as calculated by the logistic regression equation from Clabby et al (31). Although most studies on predictors of mortality are derived from databases composed predominantly of adult patients with PH, there have been several studies examining risk factors for children (14,16-19,53,54). Early studies in pediatric PH identified elevated mean RAP and a decreased stroke volume index as risk factors for increased mortality. Several more recent studies of PH registries reported poor growth, younger age, worse WHO functional class, elevated BNP, elevated uric acid, lower Qp, lower systolic blood pressure, and a higher ratio of mPAP to mean systemic arterial pressure (9,13,17,18,53) as additional risk factors. Data from the REVEAL registry confirmed several of

these variables including age at diagnosis, lower Qp, higher PVR, and poor response to acute vasoreactivity testing (14,55). PVC is an additional diagnostic tool to help monitor progression of the disease and potentially predict mortality.

Median PVC in transplant-free survivors was lower at the time of the last cardiac catheterization compared with the first catheterization. Conversely, PVC did not improve in patients with lung transplant or death. This pattern mirrors that of RAPxPVR, a metric known to be associated with survival in patients with PH. These findings may suggest that transplant-free survivors had a therapeutic response to PH treatment and were able to recruit additional functional pulmonary vasculature, while non-survivors may have had more advanced disease at diagnosis with limited vascular reserve. Thus, serial PVC measurements may be able to detect subtle improvements in vascular capacity over time and could potentially be used to monitor response to treatment.

There are multiple limitations to this study. As in the previous study by Bshouty, multiple assumptions were made that may make use of the model in other types of PH difficult. First, we assume that the lung compliance is normal for all patients, but lung compliance might be different among different pediatric patient populations. For instance, patients with bronchopulmonary dysplasia (BPD) have severely reduced lung compliance both early in life and sometimes into adulthood (56,57). We also assumed that the vascular growth of our patient population was normal. Early studies have indicated that pulmonary vascular growth and remodeling continues into childhood (58), and it is reasonable to surmise that development of pulmonary vasculature may be an ongoing process in our patients. In BPD, pulmonary vascular development can be deranged, decreasing the amount of vascular bed area (59). In this study, we excluded patients with BPD and patients under the age of four years to reduce variability in pulmonary vascular area. Future studies to examine PVC in infants and patients with BPD are warranted to determine whether this computational model correlates with hemodynamic parameters in these populations.



An additional limitation is our inclusion of patients only after data from the first cardiac catheterization is available. This excludes patients who died or underwent lung transplant prior to obtaining a cardiac catheterization, which leads to immortal time bias. Furthermore, descriptive statistics were included at time of first and last cardiac catheterization. As different patients underwent cardiac catheterizations at different times in the disease course, these comparisons do not account for the timing of the catheterization. However, survival analysis was performed later in the study using time-varying cox regression analysis, which does account for timing of cardiac catheterization.

This study was limited to assessment of PAH in children at a single institution. Our data are predominantly derived from children with Group 1 PAH including congenital heart disease-associated PAH and idiopathic PAH. Adult PAH populations are enriched with idiopathic PAH and connective tissue disorder-associated PAH (60). Whether the model will work similarly in other pediatric and adult PAH populations is unknown and warrants future studies. In addition, we will make the model program publicly available upon publication, and additional institutions will be able to assess PAH and independently assess our model.

Finally, PVC is an adjunctive tool and should not supplant other predictors and diagnostics of PAH and heart failure including PVR, mPAP, RAP, and BNP. PVC was found to be closely associated with many variables, and whether it is a better independent predictor cannot be ascertained. Nevertheless, we do believe that this adjunctive tool has the potential to improve early diagnosis and monitoring of progression of PAH.

## CONCLUSION

The computational model presented in this work used hemodynamic data and lung dimensions from pediatric patients with PAH to generate values of PVC that conformed to theoretically modeled PAH. PVC accurately predicted clinical outcomes in PAH similar to all



current predictors. Future studies are needed to confirm these observations in other patient populations and to evaluate whether PVC decreases with PH-directed therapy.

**Acknowledgements:** We would like to thank the Ayla Gunner Prushansky Research Fund for support of this manuscript.

**Sources of funding:** The project was supported by a Children's Hospital of Philadelphia Pediatric Academic Development Fund and Parker B. Francis Foundation. In addition, it was funded by K08HL140129 (DBF) and K23HL150337 (CMA).

**Disclosures:** There are no financial conflicts to disclose.

## REFERENCES

1. Chazova I, Loyd JE, Zhdanov VS, Newman JH, Belenkov Y, Meyrick B. Pulmonary artery adventitial changes and venous involvement in primary pulmonary hypertension. *Am J Pathol* 1995;146:389-97.
2. Meyrick B, Reid L. Pulmonary hypertension. Anatomic and physiologic correlates. *Clin Chest Med* 1983;4:199-217.
3. Miura A, Nakamura K, Kusano KF et al. Three-dimensional structure of pulmonary capillary vessels in patients with pulmonary hypertension. *Circulation* 2010;121:2151-3.
4. Rabinovitch M, Haworth SG, Castaneda AR, Nadas AS, Reid LM. Lung biopsy in congenital heart disease: a morphometric approach to pulmonary vascular disease. *Circulation* 1978;58:1107-22.
5. Stacher E, Graham BB, Hunt JM et al. Modern age pathology of pulmonary arterial hypertension. *Am J Respir Crit Care Med* 2012;186:261-72.
6. Tuder RM. Pathology of pulmonary arterial hypertension. *Semin Respir Crit Care Med* 2009;30:376-85.
7. McLaughlin VV, Archer SL, Badesch DB et al. ACCF/AHA 2009 expert consensus document on pulmonary hypertension a report of the American College of Cardiology Foundation Task Force on Expert Consensus Documents and the American Heart Association developed in collaboration with the American College of Chest Physicians;

- American Thoracic Society, Inc.; and the Pulmonary Hypertension Association. J Am Coll Cardiol 2009;53:1573-619.
8. Simonneau G, Montani D, Celermajer DS et al. Haemodynamic definitions and updated clinical classification of pulmonary hypertension. Eur Respir J 2019;53.
9. Bernus A, Wagner BD, Accurso F, Doran A, Kaess H, Ivy DD. Brain natriuretic peptide levels in managing pediatric patients with pulmonary arterial hypertension. Chest 2009;135:745-751.
10. Douwes JM, Hegeman AK, van der Krieke MB, Roofthoof MT, Hillege HL, Berger RM. Six-minute walking distance and decrease in oxygen saturation during the six-minute walk test in pediatric pulmonary arterial hypertension. Int J Cardiol 2016;202:34-9.
11. Miyamoto S, Nagaya N, Satoh T et al. Clinical correlates and prognostic significance of six-minute walk test in patients with primary pulmonary hypertension. Comparison with cardiopulmonary exercise testing. Am J Respir Crit Care Med 2000;161:487-92.
12. Mullen MP. Diagnostic strategies for acute presentation of pulmonary hypertension in children: particular focus on use of echocardiography, cardiac catheterization, magnetic resonance imaging, chest computed tomography, and lung biopsy. Pediatr Crit Care Med 2010;11:S23-6.
13. Ploegstra MJ, Zijlstra WMH, Douwes JM, Hillege HL, Berger RMF. Prognostic factors in pediatric pulmonary arterial hypertension: A systematic review and meta-analysis. Int J Cardiol 2015;184:198-207.
14. Barst RJ, McGoon MD, Elliott CG, Foreman AJ, Miller DP, Ivy DD. Survival in childhood pulmonary arterial hypertension: insights from the registry to evaluate early and long-term pulmonary arterial hypertension disease management. Circulation 2012;125:113-22.

15. Haworth SG, Hislop AA. Treatment and survival in children with pulmonary arterial hypertension: the UK Pulmonary Hypertension Service for Children 2001-2006. *Heart* 2009;95:312-7.
16. Manes A, Palazzini M, Leci E, Bacchi Reggiani ML, Branzi A, Galiè N. Current era survival of patients with pulmonary arterial hypertension associated with congenital heart disease: a comparison between clinical subgroups. *Eur Heart J* 2014;35:716-24.
17. Moledina S, Hislop AA, Foster H, Schulze-Neick I, Haworth SG. Childhood idiopathic pulmonary arterial hypertension: a national cohort study. *Heart* 2010;96:1401-6.
18. van Loon RL, Roofthoof MT, Delhaas T et al. Outcome of pediatric patients with pulmonary arterial hypertension in the era of new medical therapies. *Am J Cardiol* 2010;106:117-24.
19. van Loon RL, Roofthoof MT, Hillege HL et al. Pediatric pulmonary hypertension in the Netherlands: epidemiology and characterization during the period 1991 to 2005. *Circulation* 2011;124:1755-64.
20. Acosta S, Puelz C, Rivière B, Penny DJ, Brady KM, Rusin CG. Cardiovascular mechanics in the early stages of pulmonary hypertension: a computational study. *Biomech Model Mechanobiol* 2017;16:2093-2112.
21. Colunga AL, Colebank MJ, Olufsen MS. Parameter inference in a computational model of haemodynamics in pulmonary hypertension. *J R Soc Interface* 2023;20:20220735.
22. Ebrahimi BS, Tawhai MH, Kumar H et al. A computational model of contributors to pulmonary hypertensive disease: impacts of whole lung and focal disease distributions. *Pulm Circ* 2021;11:20458940211056527.
23. Tawhai MH, Clark AR, Burrowes KS. Computational models of the pulmonary circulation: Insights and the move towards clinically directed studies. *Pulm Circ* 2011;1:224-38.

24. Hunter KS, Feinstein JA, Ivy DD, Shandas R. Computational Simulation of the Pulmonary Arteries and its Role in the Study of Pediatric Pulmonary Hypertension. *Prog Pediatr Cardiol* 2010;30:63-69.
25. Kheifets VO, O'Dell W, Smith T, Reilly JJ, Finol EA. Considerations for numerical modeling of the pulmonary circulation--a review with a focus on pulmonary hypertension. *J Biomech Eng* 2013;135:61011-15.
26. Bshouty Z. Vascular compromise and hemodynamics in pulmonary arterial hypertension: model predictions. *Can Respir J* 2012;19:e15-7.
27. Bhatia SJ, Kirshenbaum JM, Shemin RJ et al. Time course of resolution of pulmonary hypertension and right ventricular remodeling after orthotopic cardiac transplantation. *Circulation* 1987;76:819-26.
28. Young JB, Leon CA, Short HD, 3rd et al. Evolution of hemodynamics after orthotopic heart and heart-lung transplantation: early restrictive patterns persisting in occult fashion. *J Heart Transplant* 1987;6:34-43.
29. Villanueva FS, Murali S, Uretsky BF et al. Resolution of severe pulmonary hypertension after heterotopic cardiac transplantation. *J Am Coll Cardiol* 1989;14:1239-43.
30. Farooqi KM, Lopez L, Pass RH, Hsu DT, Lamour JM. Reverse ventricular remodeling and improved ventricular compliance after heart transplantation in infants and young children. *Pediatr Cardiol* 2014;35:922-7.
31. Clabby ML, Canter CE, Moller JH, Bridges ND. Hemodynamic data and survival in children with pulmonary hypertension. *J Am Coll Cardiol* 1997;30:554-60.
32. Li AM, Yin J, Au JT et al. Standard reference for the six-minute-walk test in healthy children aged 7 to 16 years. *Am J Respir Crit Care Med* 2007;176:174-80.
33. Bshouty Z, Younes M. Distensibility and pressure-flow relationship of the pulmonary circulation. I. Single-vessel model. *J Appl Physiol* (1985) 1990;68:1501-13.

34. Bshouty Z, Younes M. Distensibility and pressure-flow relationship of the pulmonary circulation. II. Multibranched model. J Appl Physiol (1985) 1990;68:1514-27.
35. al-Tinawi A, Madden JA, Dawson CA, Linehan JH, Harder DR, Rickaby DA. Distensibility of small arteries of the dog lung. J Appl Physiol (1985) 1991;71:1714-22.
36. Cox RH. Comparison of mechanical and chemical properties of extra- and intralobar canine pulmonary arteries. Am J Physiol 1982;242:H245-53.
37. Karau KL, Molthen RC, Dhyani A et al. Pulmonary arterial morphometry from microfocal X-ray computed tomography. Am J Physiol Heart Circ Physiol 2001;281:H2747-56.
38. al-Tinawi A, Clough AV, Harder DR, Linehan JH, Rickaby DA, Dawson CA. Distensibility of small veins of the dog lung. J Appl Physiol (1985) 1992;73:2158-65.
39. Huang W, Yen RT, McLaurine M, Bledsoe G. Morphometry of the human pulmonary vasculature. J Appl Physiol (1985) 1996;81:2123-33.
40. Humbert M. Update in pulmonary arterial hypertension 2007. Am J Respir Crit Care Med 2008;177:574-9.
41. Humbert M, Gerry Coghlan J, Khanna D. Early detection and management of pulmonary arterial hypertension. Eur Respir Rev 2012;21:306-12.
42. Pietra GG, Capron F, Stewart S et al. Pathologic assessment of vasculopathies in pulmonary hypertension. J Am Coll Cardiol 2004;43:25s-32s.
43. Freed BH, Collins JD, François CJ et al. MR and CT Imaging for the Evaluation of Pulmonary Hypertension. JACC: Cardiovascular Imaging 2016;9:715-732.
44. Okajima Y, Ohno Y, Washko GR, Hatabu H. Assessment of pulmonary hypertension what CT and MRI can provide. Acad Radiol 2011;18:437-53.
45. Ohno Y, Koyama H, Nogami M et al. Dynamic perfusion MRI: capability for evaluation of disease severity and progression of pulmonary arterial hypertension in patients with connective tissue disease. J Magn Reson Imaging 2008;28:887-99.

46. Hislop AA, Moledina S, Foster H, Schulze-Neick I, Haworth SG. Long-term efficacy of bosentan in treatment of pulmonary arterial hypertension in children. *Eur Respir J* 2011;38:70-7.
47. Issapour A, Frank B, Crook S et al. Safety and tolerability of combination therapy with ambrisentan and tadalafil for the treatment of pulmonary arterial hypertension in children: Real-world experience. *Pediatr Pulmonol* 2022;57:724-733.
48. Ivy DD, Doran AK, Smith KJ et al. Short- and long-term effects of inhaled iloprost therapy in children with pulmonary arterial hypertension. *J Am Coll Cardiol* 2008;51:161-9.
49. Krishnan U, Takatsuki S, Ivy DD et al. Effectiveness and safety of inhaled treprostinil for the treatment of pulmonary arterial hypertension in children. *Am J Cardiol* 2012;110:1704-9.
50. Takatsuki S, Calderbank M, Ivy DD. Initial experience with tadalafil in pediatric pulmonary arterial hypertension. *Pediatr Cardiol* 2012;33:683-8.
51. Takatsuki S, Rosenzweig EB, Zuckerman W, Brady D, Calderbank M, Ivy DD. Clinical safety, pharmacokinetics, and efficacy of ambrisentan therapy in children with pulmonary arterial hypertension. *Pediatr Pulmonol* 2013;48:27-34.
52. Ten Kate CA, Tibboel D, Kraemer US. B-type natriuretic peptide as a parameter for pulmonary hypertension in children. A systematic review. *Eur J Pediatr* 2015;174:1267-75.
53. Yung D, Widlitz AC, Rosenzweig EB, Kerstein D, Maislin G, Barst RJ. Outcomes in children with idiopathic pulmonary arterial hypertension. *Circulation* 2004;110:660-5.
54. Barst RJ, Maislin G, Fishman AP. Vasodilator therapy for primary pulmonary hypertension in children. *Circulation* 1999;99:1197-208.

55. Benza RL, Miller DP, Gomberg-Maitland M et al. Predicting survival in pulmonary arterial hypertension: insights from the Registry to Evaluate Early and Long-Term Pulmonary Arterial Hypertension Disease Management (REVEAL). *Circulation* 2010;122:164-72.
56. Baraldi E, Filippone M, Trevisanuto D, Zanardo V, Zacchello F. Pulmonary function until two years of life in infants with bronchopulmonary dysplasia. *Am J Respir Crit Care Med* 1997;155:149-55.
57. Thunqvist P, Gustafsson P, Norman M, Wickman M, Hallberg J. Lung function at 6 and 18 months after preterm birth in relation to severity of bronchopulmonary dysplasia. *Pediatr Pulmonol* 2015;50:978-86.
58. Haworth SG, Hislop AA. Pulmonary vascular development: normal values of peripheral vascular structure. *Am J Cardiol* 1983;52:578-83.
59. Bourbon J, Boucherat O, Chailley-Heu B, Delacourt C. Control mechanisms of lung alveolar development and their disorders in bronchopulmonary dysplasia. *Pediatr Res* 2005;57:38r-46r.
60. Badlam JB, Badesch DB, Austin ED et al. United States Pulmonary Hypertension Scientific Registry: Baseline Characteristics. *Chest* 2021;159:311-327.



## TABLES

**Table 1. Baseline characteristics of patients**

Characteristic	Lung Transplant or Death, N = 13 <sup>1</sup>	Transplant-free survival, N = 45 <sup>1</sup>	p-value <sup>2</sup>
Sex			>0.9
Female	9 (69%)	29 (64%)	
Male	4 (31%)	16 (36%)	
Age at PAH Diagnosis (Years)	6.7 (2.6, 11.1)	4.7 (2.0, 8.0)	0.3
Age at Lung Death (Years)	17.0 (14.1, 22.5)	NA (NA, NA)	

<sup>1</sup>n (%); Median (IQR)

<sup>2</sup>Fisher's exact test; Wilcoxon rank sum test

**Table 2. Comparison of data at first catheterization from PAH patients with and without transplant-free survival**

Characteristic	N	Lung Transplant or Death, N = 13 <sup>1</sup>	Transplant-free survival, N = 45 <sup>1</sup>	p-value <sup>2</sup>
Age at Cath	58	12.7 (7.6, 14.3)	6.4 (4.9, 8.5)	0.012
BMI	58	16.85 (15.31, 17.57)	15.54 (14.46, 17.84)	0.6
BNP	38	324 (203, 1,326)	60 (30, 135)	0.010
% Pred. 6MW	32	42 (33, 59)	69 (56, 80)	0.031
QPi	57	3.65 (2.55, 5.37)	3.90 (3.30, 4.87)	0.6
mPAP	57	64 (62, 78)	34 (25, 55)	<0.001
mPCWP	56	12.5 (12.0, 15.0)	10.0 (9.0, 12.2)	0.007
PVRi	57	17 (9, 24)	6 (3, 10)	0.002
RAP	57	10.0 (7.8, 11.0)	7.0 (5.0, 9.0)	<0.001
RAPxPVRi	57	184 (66, 255)	32 (19, 68)	<0.001

<sup>1</sup>Median (IQR)

<sup>2</sup>Wilcoxon rank sum test

**Table 3. Comparison of PVC and RAP × PVC at time of first, last, and all catheterizations in PAH patients with and without transplant-free survival**

Catheterization	Characteristic	N	Lung transplant or Death, N = 13 <sup>1</sup>	Transplant-free survival, N = 45 <sup>1</sup>	p-value <sup>2</sup>
First					
	PVC	52	88 (85, 92)	77 (56, 84)	<0.001
	RAPxPVC	52	818 (617, 982)	445 (258, 583)	<0.001
Last					
	PVC	58	88 (87, 92)	66 (46, 77)	<0.001
	RAPxPVC	56	731 (576, 1,544)	363 (251, 557)	<0.001
All					
	PVC	265	88 (85, 92)	72 (58, 84)	<0.001
	RAPxPVC	259	748 (580, 959)	441 (294, 584)	<0.001

<sup>1</sup>Median (IQR)

<sup>2</sup>Wilcoxon rank sum test

**Table 4. Univariable cox regression with time varying covariates to evaluate effects of variables on time to survival**

Characteristic	N	HR <sup>1</sup>	95% CI <sup>1</sup>	p-value
Diagnosis Age	274	1.07	0.95, 1.20	0.3
Age at Catheterization	274	1.19	1.02, 1.38	0.024
BNP	237	1.00	1.00, 1.00	<0.001
% Pred. 6MW	202	0.95	0.91, 0.99	0.010
RAP	267	1.22	1.13, 1.32	<0.001
PAP	272	1.03	1.01, 1.05	0.001
LAP	271	1.09	1.01, 1.19	0.029
QPi	273	0.61	0.34, 1.08	0.092
PVRi	273	1.11	1.05, 1.18	<0.001
RAP x PVRi	267	1.00	1.00, 1.01	<0.001
PVC	265	1.10	1.02, 1.18	0.008
RAP x PVC	259	1.00	1.00, 1.00	<0.001

<sup>1</sup>HR = Hazard Ratio, CI = Confidence Interval

**Table 5. Univariate mixed model analysis of predictors of 6MW, BNP, and estimated 1-year mortality**

Dependent Variable	Characteristic	N	Beta	SE <sup>1</sup>	95% CI <sup>1</sup>	p-value
% Predicted 6MW distance	PVC	196	-0.25	0.054	-0.35, -0.14	<0.001
	PVR	201	-0.75	0.176	-1.1, -0.41	<0.001
	RAP	197	-0.96	0.295	-1.5, -0.39	0.001
	RAP x PVR	197	-0.04	0.012	-0.06, -0.02	<0.001
	RAP x PVC	192	-0.01	0.003	-0.02, -0.01	<0.001
	mPAP	200	-0.20	0.054	-0.31, -0.10	<0.001
	mLAP	199	-0.48	0.233	-0.94, -0.03	0.038
	Log QPi	201	4.9	3.16	-1.3, 11	0.12
Log BNP	PVC	265	0.12	0.028	0.07, 0.18	<0.001
	PVR	273	0.97	0.081	0.81, 1.1	<0.001
	RAP	267	2.2	0.149	1.9, 2.4	<0.001
	RAP x PVR	267	0.12	0.003	0.11, 0.12	<0.001
	RAP x PVC	259	0.02	0.001	0.02, 0.03	<0.001
	mPAP	272	0.18	0.026	0.13, 0.24	<0.001

Dependent Variable	Characteristic	N	Beta	SE <sup>1</sup>	95% CI <sup>1</sup>	p-value
Estimated 1-Year Mortality	mLAP	271	0.67	0.156	0.36, 0.97	<0.001
	Log QPi	273	-13	1.87	-17, -9.8	<0.001
	PVC	229	0.01	0.004	0.01, 0.02	<0.001
	PVR	235	0.06	0.014	0.03, 0.08	<0.001
	RAP	229	0.11	0.021	0.07, 0.15	<0.001
	RAP x PVR	229	0.00	0.001	0.00, 0.01	<0.001
	RAP x PVC	223	0.00	0.000	0.00, 0.00	<0.001
	mPAP	234	0.02	0.004	0.01, 0.03	<0.001
	mLAP	233	0.08	0.019	0.05, 0.12	<0.001
	Log QPi	235	-0.40	0.223	-0.83, 0.04	0.075

<sup>1</sup>SE = Standard Error, CI = Confidence Interval

**Table 6. Multivariable mixed model analyses of predictors of 6MW, BNP, and estimated 1-year mortality**

Dependent Variable	Model	Characteristic	Beta	SE <sup>1</sup>	95% CI <sup>1</sup>	p-value
Estimated 1-year mortality	12	PVR	0.78	0.093	0.60, 0.96	<0.001
	12	RAP	1.9	0.189	1.6, 2.3	<0.001
	12	% Pred. 6MW	0.12	0.039	0.04, 0.19	0.003
	12	Log BNP	-0.40	0.445	-1.3, 0.47	0.4
	12	Log QPi	-4.1	1.47	-7.0, -1.2	0.005
Estimated 1-year mortality	13	PVC	0.08	0.033	0.01, 0.14	0.017
	13	RAP	2.3	0.218	1.8, 2.7	<0.001
	13	% Pred. 6MW	0.06	0.047	-0.04, 0.15	0.2
	13	Log BNP	-0.03	0.548	-1.1, 1.0	>0.9
	13	Log QPi	-6.9	1.80	-10, -3.3	<0.001

<sup>1</sup>SE = Standard Error, CI = Confidence Interval

## FIGURE LEGENDS

**Figure 1. Computed pulmonary vascular compromise (PVC) versus changes in mean pulmonary artery pressure (mPAP) in simulated pulmonary arterial hypertension (PAH) and in a pediatric PAH patient population.** (A) PVC in simulated PAH calculated using a stepwise increase in mPAP in mmHg and either a pulmonary blood flow (Qp) of 2.5 L/min or 7.5 L/min. (B) PVC in a pediatric PAH study group calculated similarly and divided into three groups of indexed pulmonary blood flow (Qpi) in L/min/m<sup>2</sup>. Lorentzian curve fitting used to generate trendlines.

**Figure 2. Computed PVC versus changed in indexed pulmonary vascular resistance (PVRi) in simulated PAH and in a pediatric PAH patient population.** (A) PVC in simulated PAH calculated using a stepwise increase in PVR in Wood units and either a pulmonary blood flow (Qp) of 2.5 L/min or 7.5 L/min. (B) PVC versus PVRi in pediatric PAH study group

calculated similarly and divided into three groups of indexed pulmonary blood flow (Qpi) in L/min/m<sup>2</sup>. Lorentzian curve fitting used to generate trendlines.

**Figure 3. Computed PVC in pediatric patients with PAH and patients with WHO Group 2 pulmonary hypertension. (A) PVC vs. mPAP. (B) PVC vs. PVRi.**

**Figure 4. Improvement in pulmonary vascular compromise over time following orthotopic heart transplantation in a pediatric patient with WHO group 2 pulmonary hypertension.**

**Figure 5. Kaplan-Meier survival estimates for transplant-free survival at last cath. (A) 10-year survival for PVC > 80% is 54% (95% CI 35%, 81%),  $p < 0.001$ . (B) 10-year survival for PVRi > 8 iWU is 61% (95% CI 44%, 85%),  $p < 0.001$ . (C) 10-year survival for mPAP  $\geq$  42 mmHg is 60% (95% CI 43%, 84%),  $p < 0.001$ . (D) 10-year survival for RAPxPVC > 510 is 66% (95% CI 49%, 88%),  $p = 0.002$ . (E) 10-year survival for BNP > 65 pg/mL is 68% (95% CI 51%, 91%),  $p = 0.036$ . (F) 10-year survival for percent predicted 6-minute walk distance  $\leq$  72% is 59% (95% CI 40%, 88%),  $p < 0.001$ . Lung transplant or death (n = 13) and transplant-free survival (n = 45).**



Figure 1.

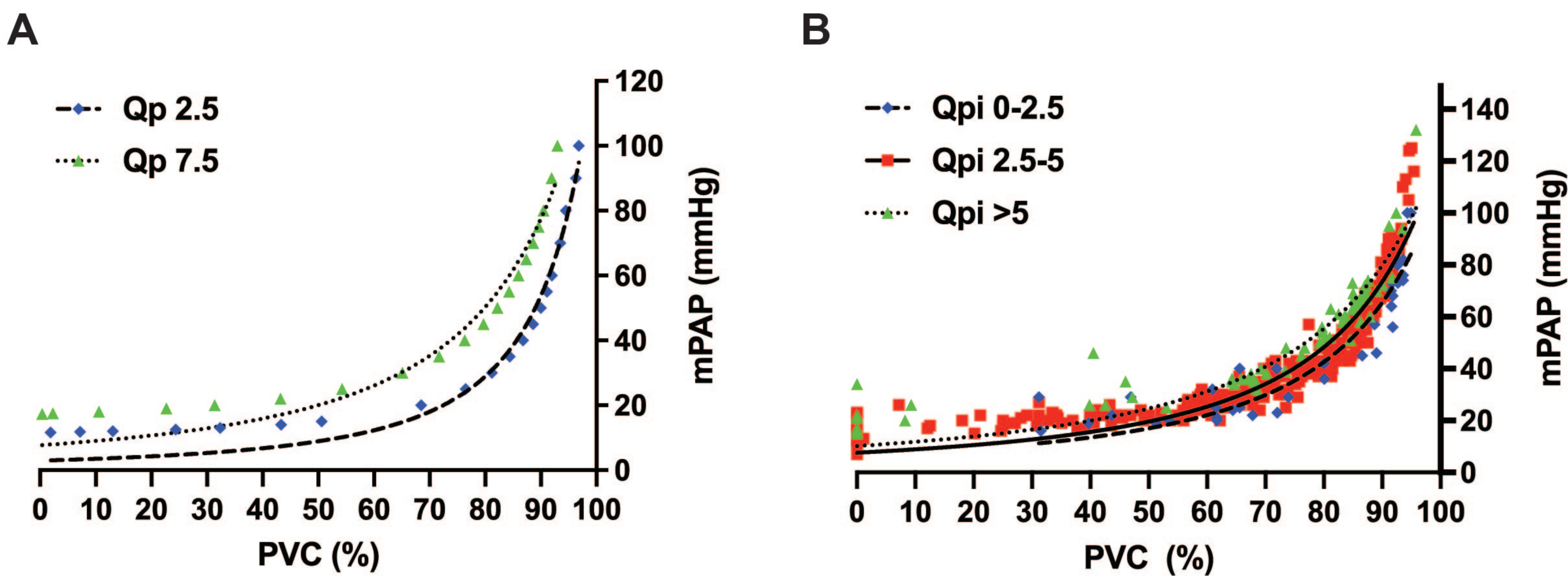
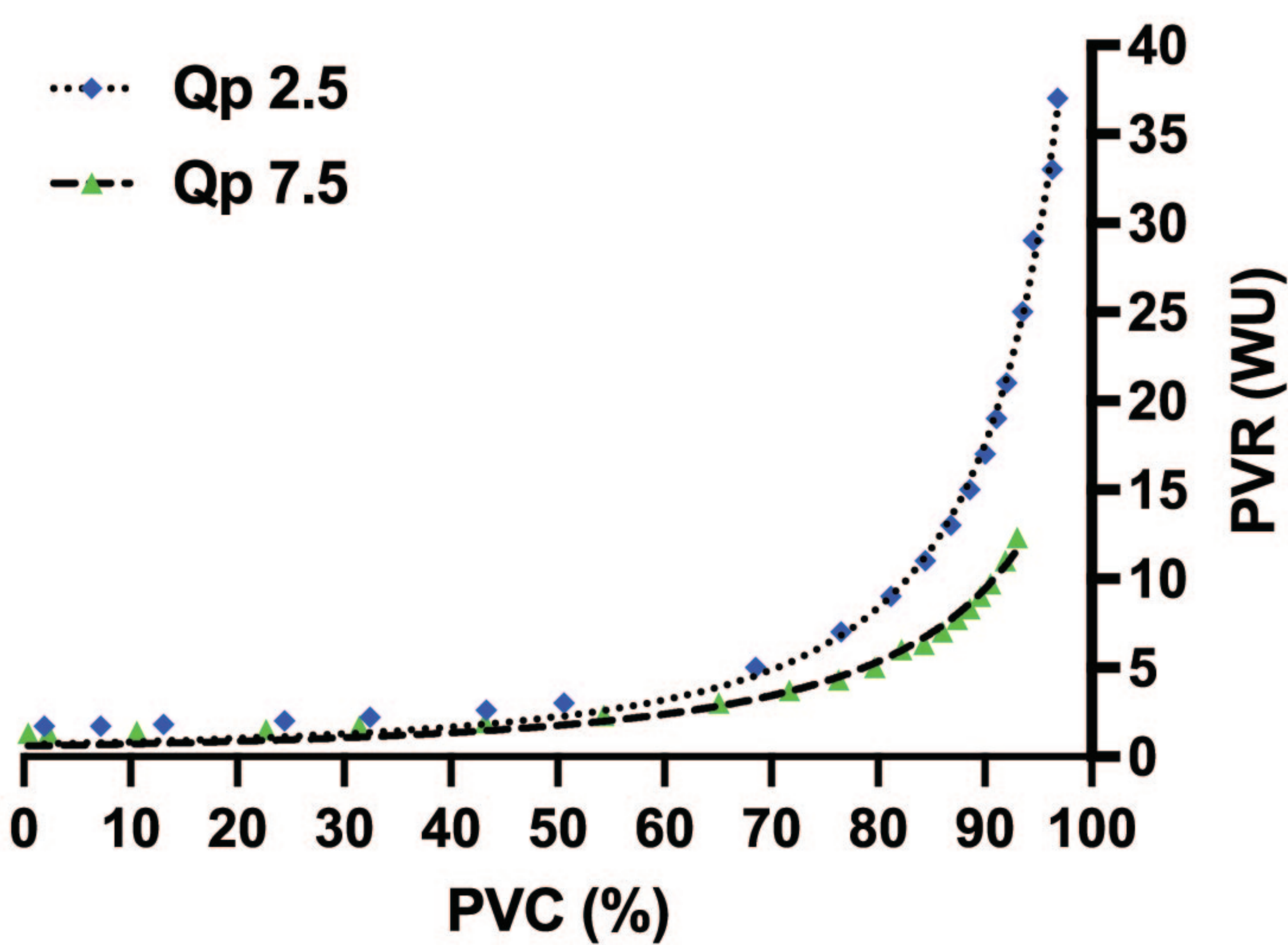


**Figure 1. Computed pulmonary vascular compromise (PVC) in simulated pulmonary arterial hypertension (PAH) and in a pediatric PAH patient population.** (A) PVC in simulated PAH calculated using a stepwise increase in mean pulmonary artery pressure (mPAP) in mmHg and either a pulmonary blood flow (Qp) of 2.5 L/min or 7.5 L/min. (B) PVC in a pediatric PAH study group calculated similarly and divided into three groups of indexed pulmonary blood flow (Qpi) in L/min/m<sup>2</sup>. Lorentzian curve fitting used to generate trendline

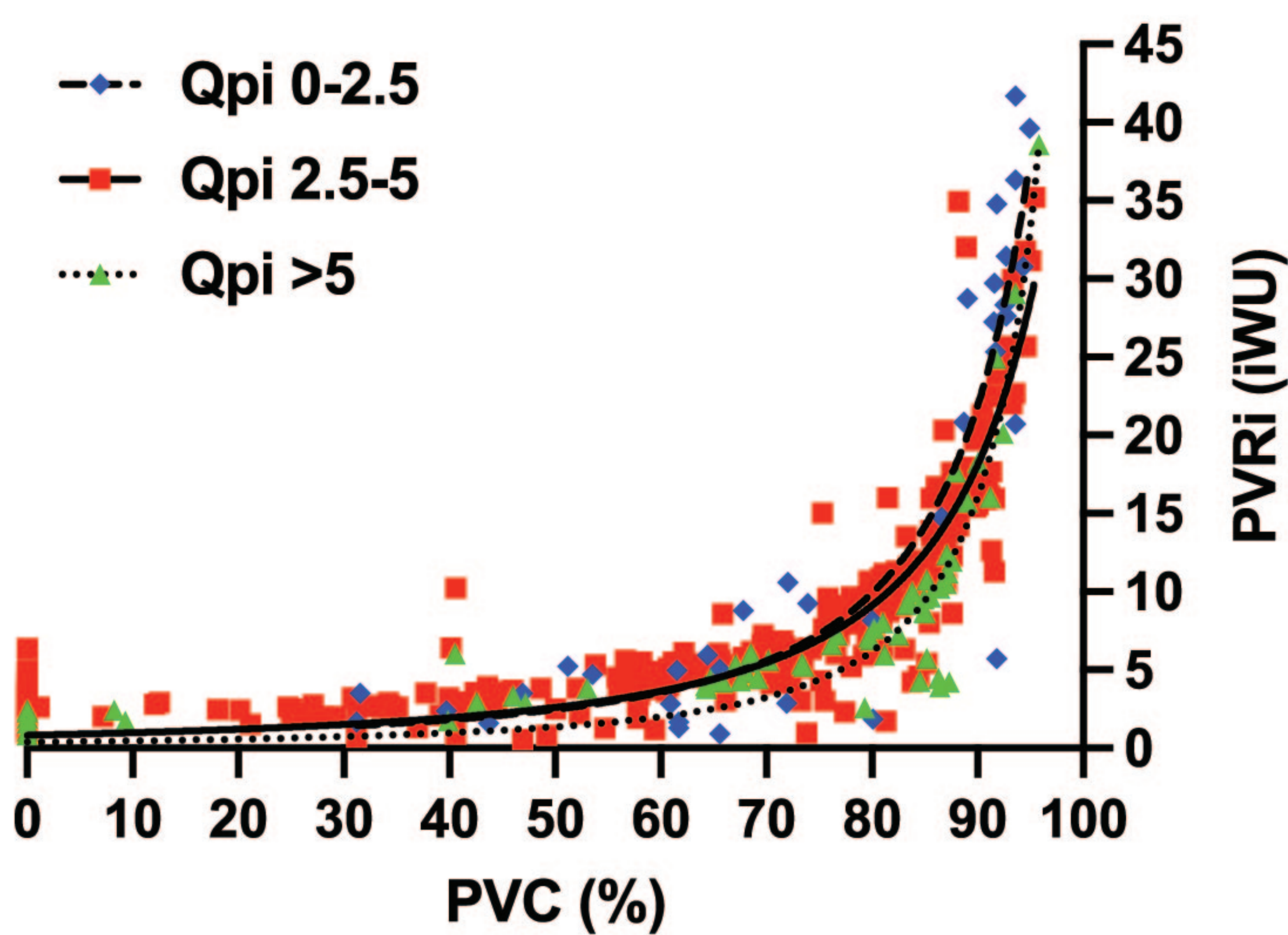


Figure 2.

A



B

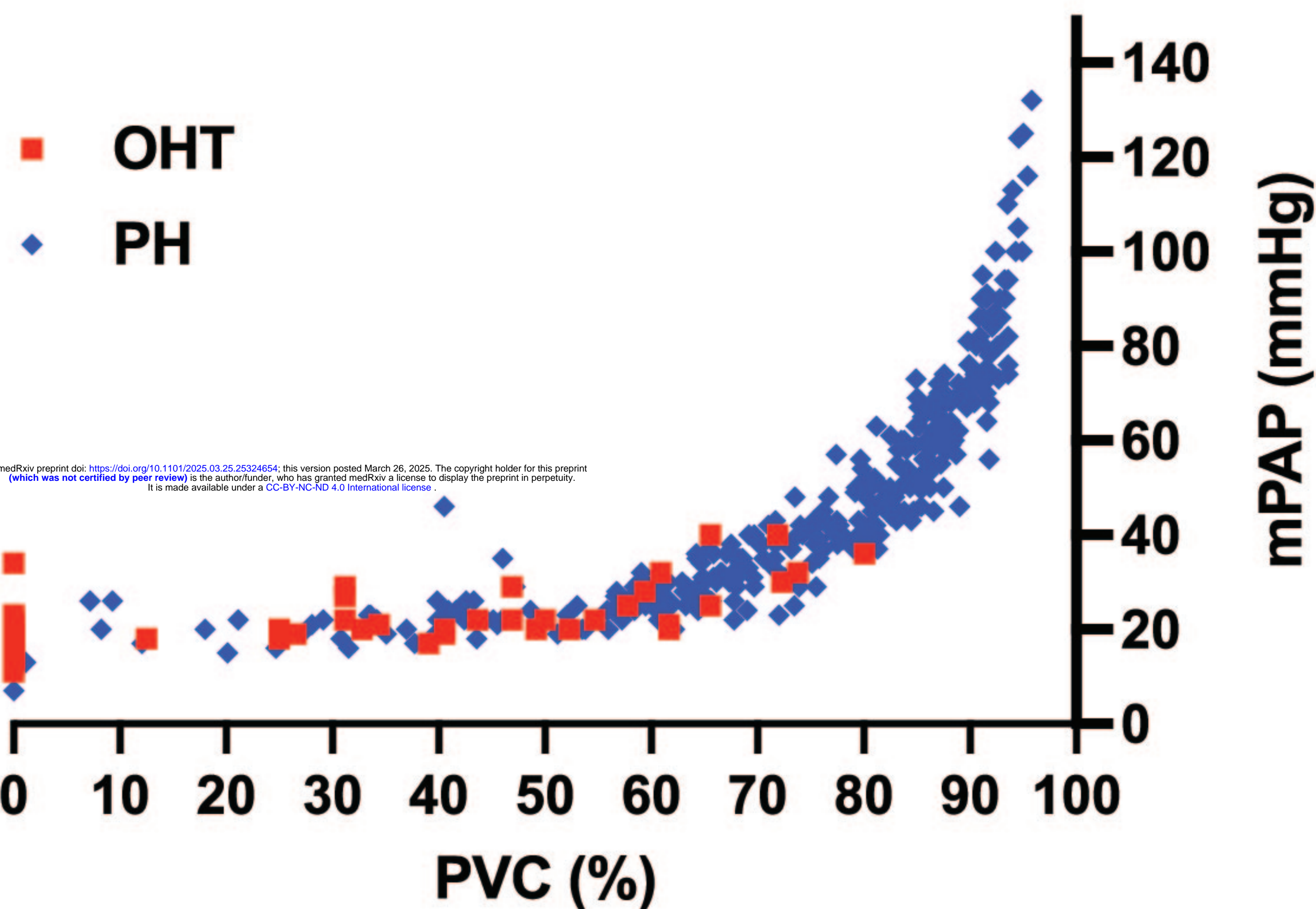


**Figure 2. Computed pulmonary vascular compromise (PVC) in simulated pulmonary arterial hypertension (PAH) and in a pediatric PAH patient population.** (A) PVC in simulated PAH calculated using a stepwise increase in pulmonary vascular resistance (PVR) in Wood units and either a pulmonary blood flow ( $Q_p$ ) of 2.5 L/min or 7.5 L/min. (B) PVC in pediatric PAH study group calculated similarly and divided into three groups of indexed pulmonary blood flow ( $Q_{pi}$ ) in L/min/m<sup>2</sup>. Lorentzian curve fitting used to generate trendline



Figure 3.

A



B

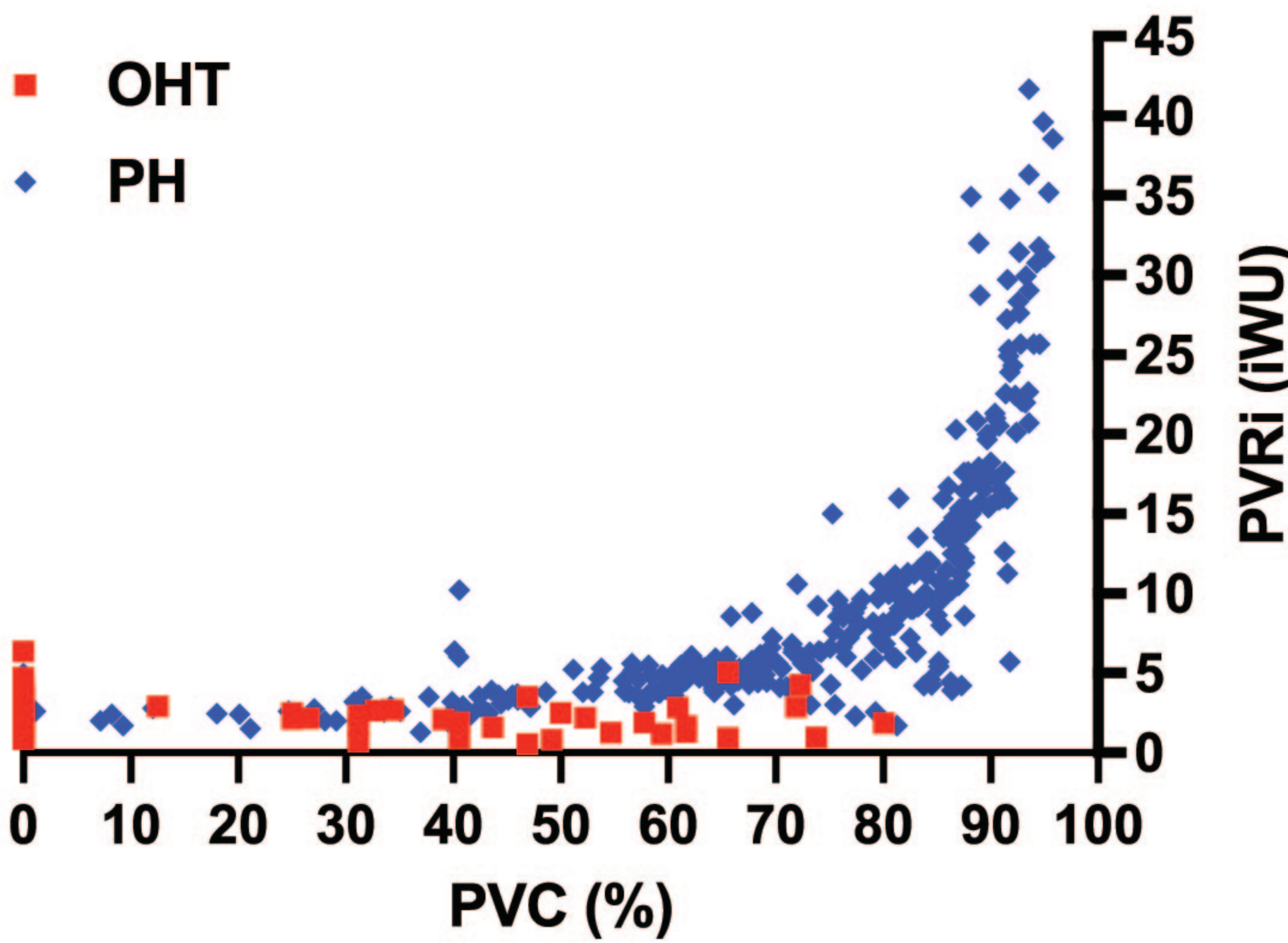


Figure 3. Computed pulmonary vascular compromise (PVC) in pediatric patients with pulmonary arterial hypertension and patients with pulmonary hypertension associated with left-sided heart disease. (A) PVC vs. mean pulmonary artery pressure (mPAP). (B) PVC vs. indexed pulmonary vascular resistance (PVRI).



Figure 4.

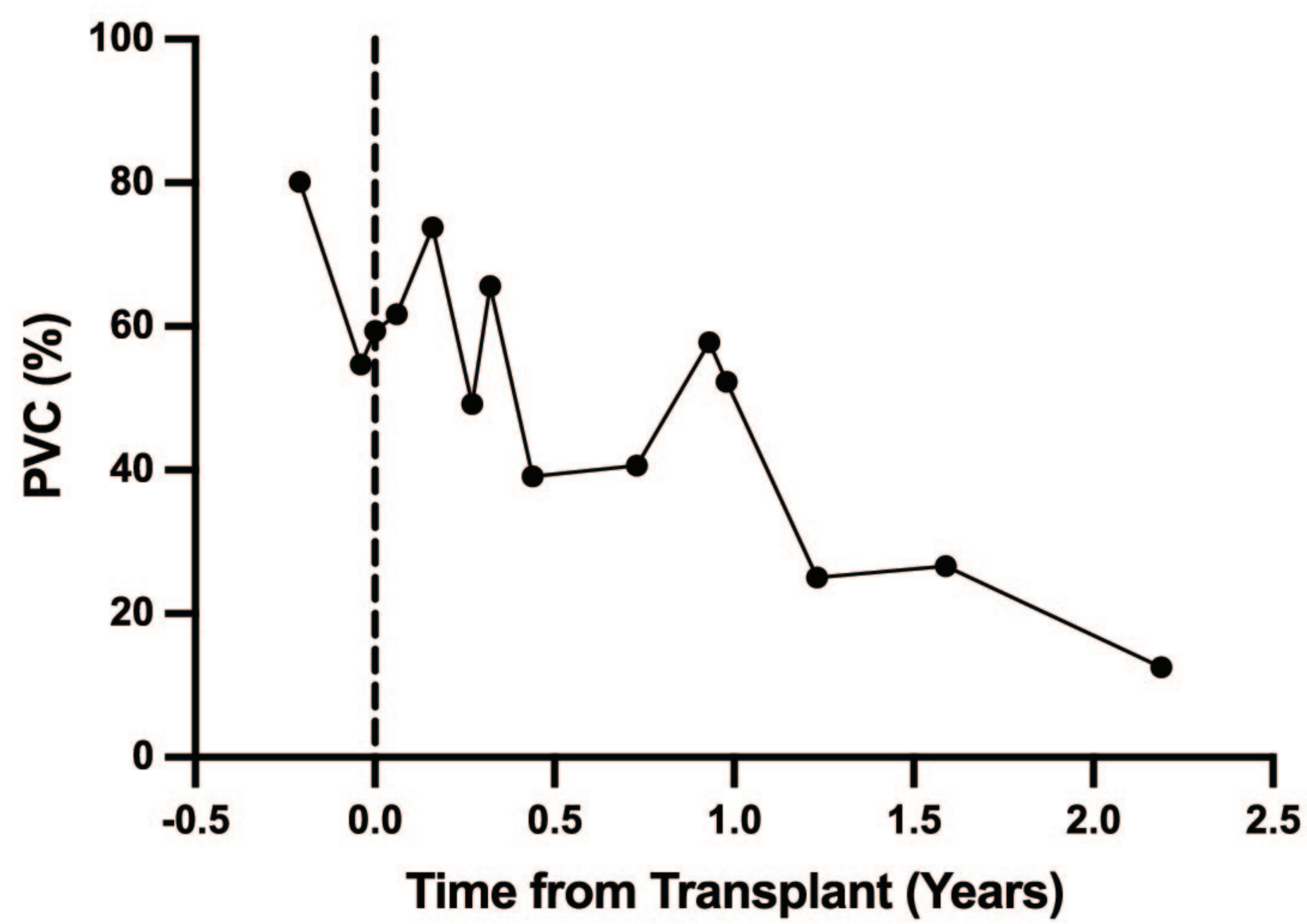
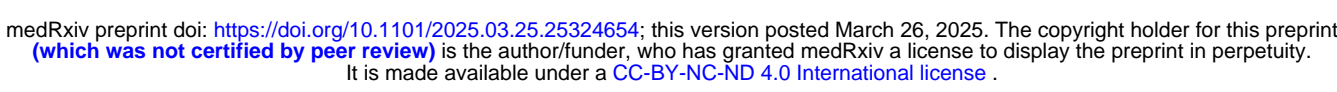


Figure 4. Improvement in pulmonary vascular compromise over time following orthotopic heart transplantation in a pediatric patient with World Health Organization group 2 pulmonary hypertension.



# A



al for percent predicted 6-minute walk distance  $\leq 72\%$  is 59% (95% CI 40%, 88%),  $p < 0.001$ .